

Plasmonic Nanohole Arrays for Real-Time Multiplex Biosensing

Antoine Lesuffleur, Hyungsoon Im, Nathan C. Lindquist, Kwan Seop Lim, and Sang-Hyun Oh*
Laboratory of Nanostructures and Biosensing, Department of Electrical and Computer Engineering
University of Minnesota, Twin Cities, 200 Union St. SE, Minneapolis, MN 55455, U.S.A.

ABSTRACT

Large-scale studies of biomolecular interactions required for proteome-level investigations can benefit from a new class of emerging surface plasmon resonance (SPR) sensors: nanohole arrays and surface plasmon (SP) enhanced optical transmission. In this paper we present a real-time, label-free multiplex SPR imaging sensor in a microarray format. The system presented is built around a low-cost microscope with laser illumination, integrated with microfluidics. The specific binding kinetics of biotin and streptavidin are measured from several sensing elements simultaneously, demonstrating the feasibility of using nanohole arrays as a high-throughput SPR microarray sensor.

Keywords: Surface plasmon resonance imaging, periodic nanohole arrays, real-time label-free biosensing, plasmonics

1. INTRODUCTION

Surface plasmon resonance (SPR) is the gold standard for real-time, label-free measurements of biomolecular interactions and plays an important role in drug discovery, systems biology and proteomics research [1,2]. In this technique, molecules immobilized on a gold surface are contacted by an aqueous buffer containing ligands, and changes in the local refractive index due to the bound ligands are detected as a shift in the SPR excitation angle or wavelength. Surface plasmons (SPs) are electromagnetic waves that are coupled to the free electron plasma in a metal [3]. Because of this coupling, SP waves exist only at the interface between a metallic film and a surrounding dielectric medium, such as water. The SP electromagnetic field decays away exponentially from the metal surface, meaning that most of its energy is confined to within ~ 100 nm of the surface, making its resonance properties very sensitive to the presence of any changes in the local refractive index. Since SPs are coupled to free electrons, for a given frequency (or energy) they have a larger wavevector (or increased momentum) than free-space electromagnetic waves, necessitating various geometries to increase the wavevector of the exciting light, such as the use of an optical prism or grating.

In commercial SPR instruments, e.g. BIAcoreTM, a convergent light cone illuminates the detection spot on a gold film via prism coupling in total internal reflection mode, known as the Kretschmann configuration. The angular distribution of the reflected light is measured by a photodiode array in real-time, scanning for a steep drop in intensity that indicates the resonant excitation of SPs. This gives a local refractive index sensitivity of $\Delta n/n \sim 10^{-6}$ [4]. Using this real-time, label-free method, binding kinetics (association/dissociation rates and equilibrium constants) can be precisely measured using a smaller sample volume than other equilibrium measurement techniques. In various formats, the technique has found wide applications in pharmaceutical development as well as in basic research.

For large-scale studies of protein-protein or protein-nucleic acid interactions on a microarray [5], a new class of high-throughput instrument is desired that is capable of simultaneously measuring thousands of molecular interactions using a simple and affordable setup. SPR microscopy provides one path to multiplex SPR sensing, wherein a refractive index variation across a sample surface, e.g. a microarray, due to molecular binding events is translated into a contrast distribution in the image plane [6,7]. While many research groups have successfully demonstrated SPR imaging using the Kretschmann configuration [8-11], the coupling prism in that setup results in a tilted image plane, prohibiting the use of high numerical aperture (NA) optics with a limited depth-of-field. This limits the size of a microarray that can be imaged with high quality. A commercial FlexchipTM instrument [12] instead utilizes a higher order diffracted mode of a grating coupler for SPR excitation and can measure binding kinetics from 400 sample spots simultaneously. However, the issues associated with a tilted image plane still persist, and its high cost is a barrier to widespread use. Recently, a new class of high-throughput SPR microarray sensing has emerged as an attractive alternative to prism or grating based systems, based on the extraordinary optical transmission (EOT) effect through periodic nanohole arrays [13-22]. In this work, we describe the potential of a periodic nanohole-based SPR sensor to simplify the imaging setup, increase the microarray packing density, and enable the use of a stable laser source and high-resolution imaging.

*E-mail: sang@umn.edu; phone 1-612-625-0125; <http://nanobio.umn.edu>

2. PERIODIC NANO HOLE ARRAYS AS REAL-TIME LABEL-FREE SPR SENSORS

2.1 Extraordinary optical transmission (EOT) through subwavelength apertures

Ebbesen et al. discovered that light transmission through periodic sub-wavelength hole arrays milled through a thin gold or silver film could be more efficient than predicted by conventional theories [23]. Subsequent work has shown that surface plasmons (SPs) excited via grating (periodic array) coupling on both sides of the metal film resonate through the nanoholes as if in an optical cavity, enhancing the light transmission at specific wavelengths depending on the periodicity of the array and the dielectric function of both the metal and the surrounding dielectric [24]. Since more light energy is transmitted than is incident on the open hole area, this phenomenon is called the extraordinary optical transmission (EOT) effect. For a square array of circular nanoholes optically excited at normal incidence, the positions of the transmission peaks λ_{SP} can be approximated by the following equation:

$$\lambda_{SP}(i,j) = \sqrt{\frac{\epsilon_d \epsilon_m}{\epsilon_d + \epsilon_m}} \cdot \frac{P}{\sqrt{i^2 + j^2}}, \quad (1)$$

where P is the periodicity of the array, the integers (i, j) represent the Bragg resonance orders, and ϵ_m and ϵ_d are the dielectric functions of the metal and surrounding dielectric medium, respectively. It should be noted that experimentally measured peak positions are slightly red-shifted from those predicted by Eq. 1 due to interference between direct transmission through the holes and the resonant excitation of SP modes [25,26]. With regard to the exact role of SPs, the mechanism responsible for EOT has been a hotly debated topic [27-29]. Theoretical and experimental work from several groups now seem to converge on the idea that SPs do play a central role in enhancing the transmission [30]. Similar enhanced transmission effects were also intensely studied for isolated subwavelength slits or slit arrays, showing that the transmission efficiency normalized by the slit area can be well over 100 % [31].

Figure 1a shows a sample nanohole array fabricated on a gold film on a glass slide (refer to section 3 for fabrication details). When light is incident from the glass side, SPs are resonantly excited on both surfaces of the film, boosting the transmission. Figure 1b shows finite-difference time-domain (FDTD) simulations of the SP field, i.e. the electric field component perpendicular to the metal surface. Since the field is confined very close to the metal film (within ~100 nm), the SP mediated transmission properties are very sensitive to the presence of any molecular layers on the surface. Figure 1c shows the transmission spectrum of a sample nanohole array, with SP enhanced transmission peaks near 675 nm and 550 nm.

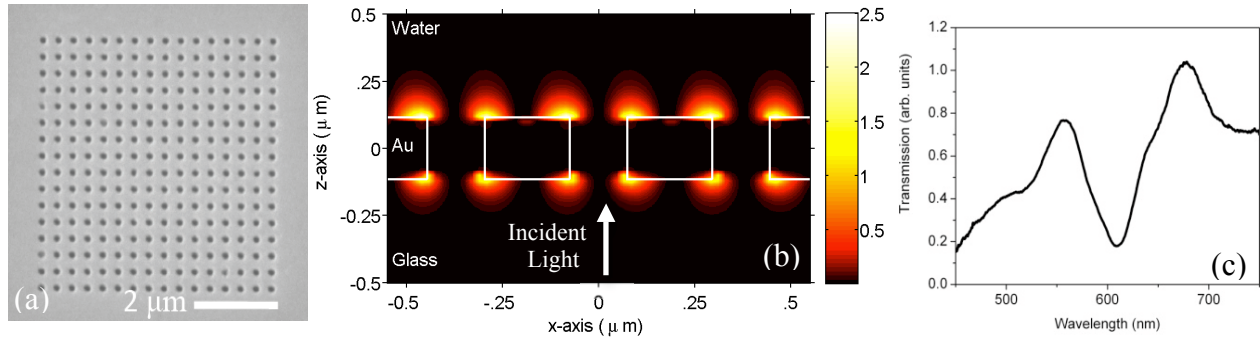


Fig. 1. a) SEM image of a nanohole array in a gold film. b) FDTD calculations for a 370 nm periodicity and a 150 nm hole diameter nanohole array. c) Transmission spectrum from a nanohole array with a 390 nm periodicity and a 150 nm hole diameter.

2.2 Periodic nanohole arrays for SPR biosensing

BIAcore™ instruments measure the changes in the SPR excitation angle due to refractive index changes near the metal-dielectric interface. Likewise, since λ_{SP} in Eq. 1 depends on the refractive index near the surface of a gold film (viz. ~100 nm), periodic nanohole arrays can be used for refractive index sensing with a high signal-to-noise ratio. Brolo et al. first demonstrated periodic nanohole arrays in a gold film for refractive index sensing [13]. They used 200 nm diameter holes with periodicities ranging from 510 nm to 618 nm. Their experiments consisted of measuring the spectra of the nanohole arrays before and after molecular binding events using a broadband light source and a spectrometer.

They reported a 4 nm shift of the EOT peaks after the immobilization of a molecular monolayer on a gold surface [13]. They also presented biotin-streptavidin specific binding [17]. Tetz et al. demonstrated refractive index sensing using periodic nanoholes (200 nm hole diameter and 1400 nm periodicity) with a tunable IR laser source (1520-1570 nm) and estimated the sensing limits to be close to 10^{-6} , comparable with conventional BIAcore™ instrumentation [16]. Recently, we demonstrated real-time measurements of molecular binding using shape-enhanced nanohole arrays in a flow cell [18]. For this work, we used arrays of apertures consisting of two overlapping circular holes to produce sharp apices (figure 2a) and demonstrated a 50% improvement in sensitivity. A real-time measurement of bovine serum albumin (BSA) adsorption on the gold surface was also presented and is shown in figure 2b. Pang et al. studied theoretically and experimentally the sensitivity of nanohole arrays and measured binding kinetics between BSA and monoclonal anti-BSA [19]. Enhanced transmission through metal meshes was also observed in mid-infrared regions, which are important regions for biochemical sensing applications [14, 21].

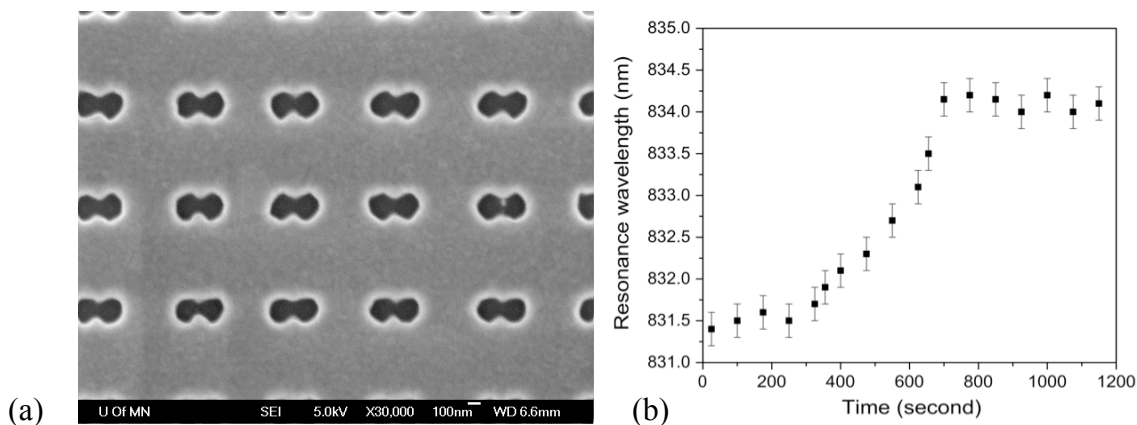


Fig. 2. a) SEM image of a double-hole array. b) Real-time measurement of BSA adsorption on the gold surface [18].

While a spectrometer or a tunable laser source can be used to scan and precisely measure the EOT changes before and after molecular binding, it cannot be easily implemented in a high-throughput manner for hundreds or thousands of sample spots on a microarray. Tunable lasers also increase the cost of the system. The multiplexing scheme demonstrated in section 4 uses a single wavelength laser source, a microscope and a CCD or CMOS camera, providing a more practical option for high-throughput SPR imaging in large-scale microarray format.

3. REAL-TIME SPR MICROARRAY IMAGING WITH LASER-ILLUMINATED NANO HOLE ARRAYS

3.1 Multiplex SPR sensing using periodic nanohole arrays

While SPR imaging or SPR microscopy has been mostly demonstrated using the Kretschmann setup, the concept can be applied equally well to periodic nanohole arrays. Lesuffleur et al. demonstrated real-time multiplex SPR sensing with periodic nanohole arrays to detect the formation of a self-assembled monolayer (SAM) on a gold surface [20]. There, instead of measuring the EOT spectra, the transmitted light intensity from each nanohole array is simultaneously recorded using a CCD or CMOS camera in real-time. Nanohole arrays provide unique advantages compared to the Kretschmann configuration by eliminating the bulky coupling prism and many optical problems associated with it for multiplex imaging [32]. In the Kretschmann SPR imaging setup, an incident beam illuminates the sensing surface at a sizeable tilt angle, causing the reflected beam to have a wide range of focal depths depending on the spatial position on the image plane of each sensor element. Furthermore, the aberration due to varying optical path lengths (glass thickness) caused by the prism limits the lateral size of the object, e.g. a microarray that can be imaged with high quality. SPR imaging sensors on a flat gold surface suffer from coherent noise and interference patterns when an expanded laser beam is used to illuminate the surface, making it difficult to image the sample surface with high resolution. Because a periodic nanohole array can directly couple incident light into SPs via grating coupling, it can significantly simplify the optical imaging setup. In this regard, nanohole array SPR sensors are similar to the Flexchip™ system, which also uses grating coupling for SPR excitation. However, the Flexchip™ uses a non-zero diffraction order, which still shares the problems of a tilted image plane discussed previously. In addition to eliminating the coupling prism, nanohole arrays bring a number of other key advantages to microarray-based SPR imaging: the small footprint of each sensing element (<10 μm

in width) allows massive parallelism and significantly reduced sample consumption, the possibility of using high NA optics for improved imaging resolution, and simplified co-linear alignment with normally incident optical excitation. Furthermore, the high intensity and stability of a laser source offers an inherent advantage over an LED or halogen source in reducing the influence of shot noise and source fluctuation, making this approach compelling for high-sensitivity, high-resolution, high-throughput SPR imaging. Laser illumination also opens up the possibilities of using various interferometric techniques for SPR sensing.

3.2 Theoretical Motivation

For multiplex SPR imaging, the intensity of the transmitted light I_T is directly dependent upon the wavelength at which the laser samples the transmission resonances of each nanohole array. Figure 3a shows FDTD simulations of several transmission spectra from a nanohole array as the refractive index of the surrounding medium is changed from that of water to that of ethanol. As the refractive index increases, the transmission peak red-shifts, per equation (1), and the intensity I_T at a fixed wavelength changes. In this manner, real-time refractive index changes can be measured from each nanohole array sensing element. Figure 3b shows the transmitted intensity at 633 nm, where the slope of the transmission peak is large and positive, leading to a sharp drop in intensity.

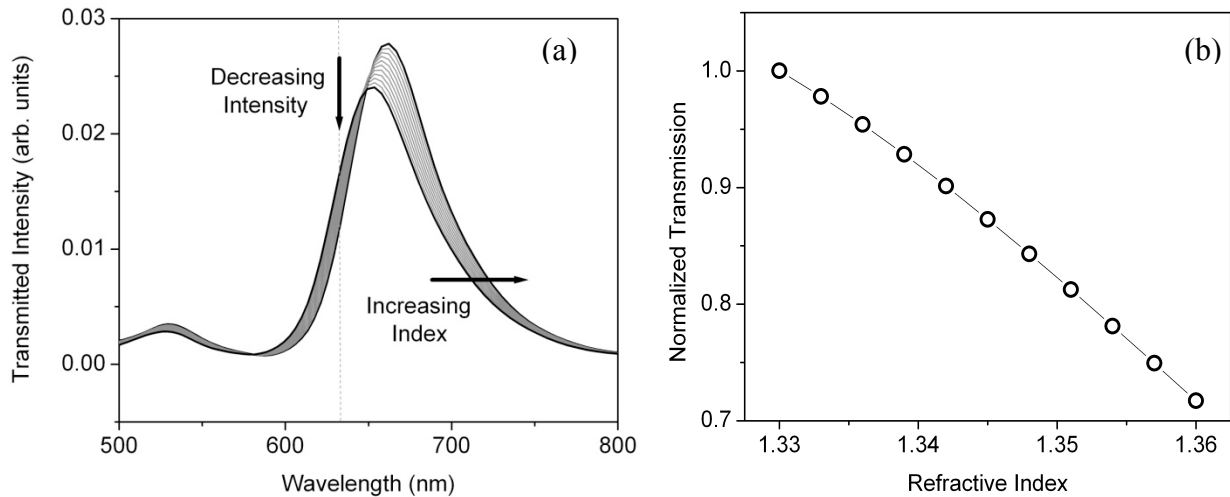


Fig. 3. (a) FDTD calculations of the transmitted intensity through a nanohole array with a 370 nm periodicity and incubated in various media with refractive indices varying from 1.33 to 1.36 (b) By sampling the transmission at 633 nm, the intensity is seen to decrease as the refractive index increases.

Mathematically, this change in intensity can be expressed as follows:

$$\Delta I_T = -(dI_T / d\lambda) \cdot S(\Delta n), \quad (2)$$

where $(dI_T / d\lambda)$ represents the slope of the transmission resonance and $S(\Delta n)$ represents the spectral shift per bulk refractive index change. For a molecular layer, Δn is represented by an effective change in refractive index, which depends on the layer refractive index, the layer thickness, and the probing range of the exponential SP field, i.e. its decay length [33]. Expressed mathematically:

$$\Delta n = (n_{molecule} - n_{buffer}) \cdot (1 - e^{-2d/l_d}) \quad (3)$$

where $n_{molecule}$ and n_{buffer} are the refractive indices of the molecule and the buffer, d is the thickness of the molecular layer, and l_d is the decay length of the exponential SP field. A fundamental characteristic of SPR sensors can be emphasized here: thin molecular layers (of a few nm) are best probed by SPs with shorter decay lengths. This is partly achievable by using shorter excitation wavelengths (like 633 nm) or by optimizing the shape of the nanoholes, as shown in figure 2a, and demonstrated in [18].

Since the imaging sensitivity depends on the sharpness of the resonance, it is important to tune the periodicity of the nanohole arrays such that the region with the highest slope is at the wavelength of the excitation source in the buffer. For

small changes in resonance wavelength, the high-slope region of the transmission spectrum is linear, and the variation of the transmitted laser intensity can be directly connected to the kinetic trend of specific molecular binding.

4. EXPERIMENTAL TECHNIQUES AND RESULTS

4.1 Nanofabrication and microfluidic integration

For fabrication, standard glass slides were sequentially cleaned with acetone, methanol, isopropyl alcohol and deionized water in ultrasonic baths for 15 minutes each. An e-beam evaporator (CHA. SEC600) was used to deposit a 5 nm chromium adhesion layer and a 200 nm gold film on the glass slides. Nanohole arrays were patterned with focused ion beam milling (FIB) using a 30kV and 30 pA ion beam (FEI Dual Beam Quanta 200 3D). A typical sensing element, as shown in figure 1a, consisted of a 16X16 nanohole array with a footprint of $40 \mu\text{m}^2$. The nanohole array periodicities ranged between 380 nm and 420 nm with an error of ± 10 nm.

Soft lithography [34] with polydimethylsiloxane (PDMS) was used to fabricate a microfluidic flow cell for real-time SPR sensing. The negative-tone master mold of the channel was patterned on a silicon wafer using SU-8 photoresist, defining 50 μm deep and 100 μm wide channels (Figure 4a). A 10:1 ratio of PDMS and curing agent was cast on the photoresist pattern (Figure 4b). After curing the PDMS at 80° C overnight, the PDMS flow cell was aligned to the nanohole arrays on a sample slide using a Karl Suss MJB3 contact aligner (Figure 4c). The surfaces of the PDMS channel and the sample slide were treated with an O₂ plasma and covalently bonded to seal the flow channel (Figure 4d).

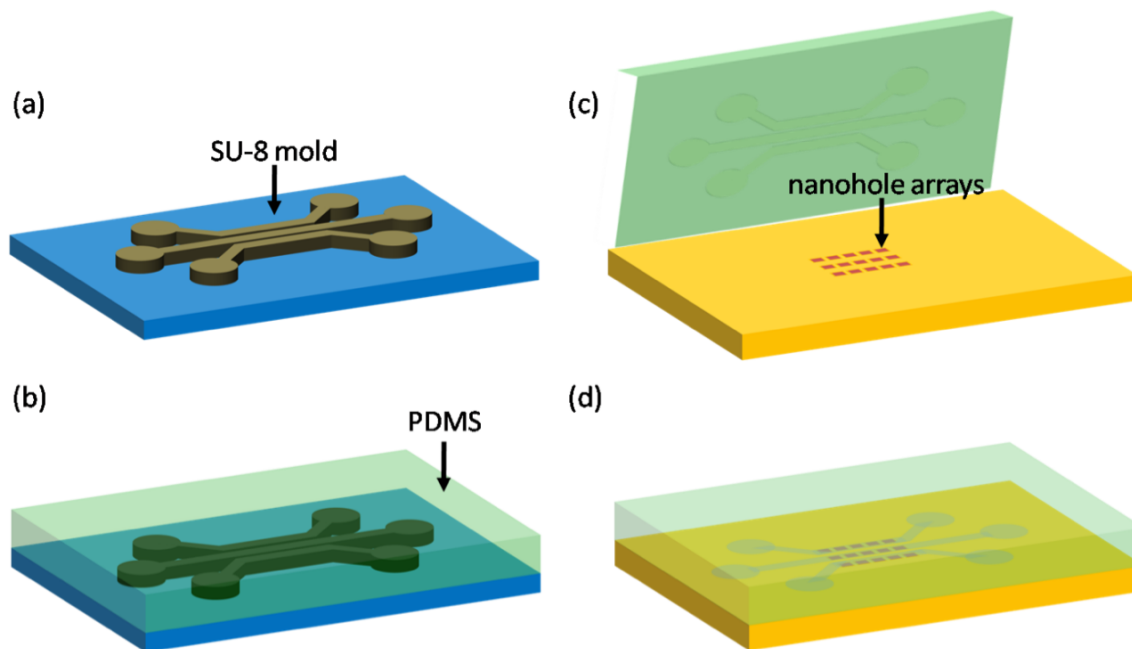


Fig. 4. Microfluidic fabrication process. (a) Master mold fabrication with SU-8 photoresist on a silicon wafer. (b) Curing PDMS over the master mold. (c) Alignment of the PDMS microfluidic channels to the nanohole arrays after O₂ plasma treatment. (d) Permanently bonded microfluidic chip.

4.2 Instrumentation and real-time data acquisition

As shown in figures 5a and 5b, the system setup is based on a standard upright microscope. A HeNe laser illuminates the bottom surface of the nanohole arrays, exciting SPs and the EOT effect. For real-time measurements of surface chemistry events, a deep-cooled CCD camera (Photometrics CoolSNAP HQ²) was used to sequentially capture images from the periodic nanohole microarray, and a syringe pump (Harvard apparatus PHD2000) was used to inject sample solutions at a flow rate ranging from 2 $\mu\text{L/hr}$ to 100 $\mu\text{L/min}$. A custom-built MATLABTM suite of analytical and signal processing code was used to control the CCD camera, capture image files at regular intervals of several seconds to several minutes, and process the image data to extract intensity profiles across the periodic nanohole microarray. For

each image captured, rapid multi-frame averaging was used to increase the signal-to-noise. The response of a single sensor spot was quantified by integrating the transmitted intensity through each nanohole array.

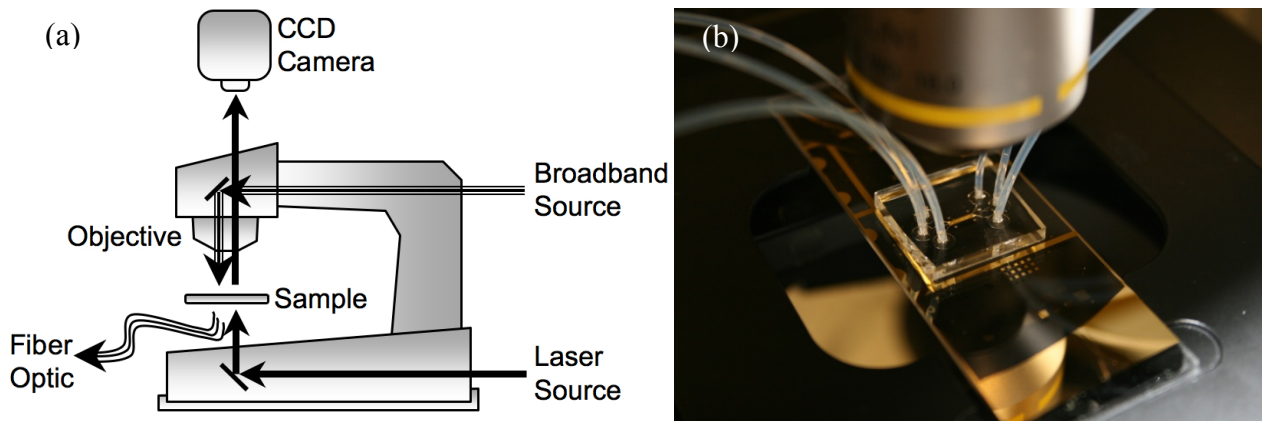


Fig. 5. (a) Schematic of the measurement system, showing a broadband lamp for spectral measurements and bright-field image capture, and the laser source for real-time multiplex SPR imaging. (b) Image of the microfluidic chip on the microscope stage.

4.3 Tuning nanohole periodicity for optimal sensitivity

Figure 6a shows a bright-field CCD image in reflection mode of several nanohole arrays with different periodicities and hole diameters. Figure 6b shows the CCD image in transmission mode of the same sample illuminated by a HeNe laser (633 nm). In figure 6b, one can see that larger hole diameters transmit more light. Also, periodicities of 380 nm and 390 nm transmit more light at 633 nm than a periodicity of 420 nm.

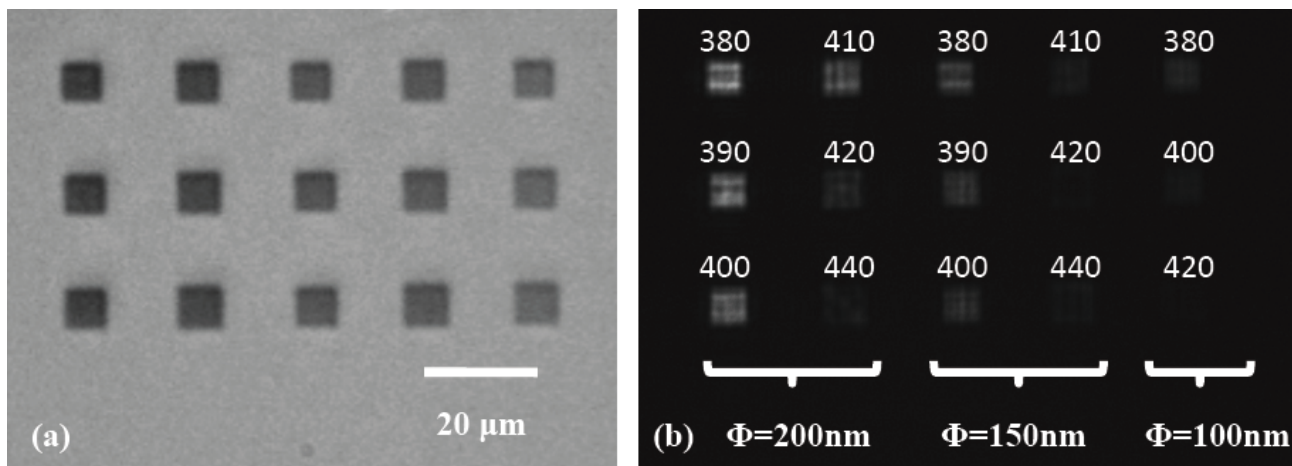


Fig. 6. CCD images of arrays with various hole diameters and periodicities. a) Bright field image in reflection mode and b) image in transmission mode using a 50× microscope objective. The arrays are illuminated by a 633nm HeNe laser beam.

4.4 Multiplex microarray sensing using periodic nanohole arrays

Figure 7a presents a bright-field CCD image of the device used for real-time protein-protein measurements. Three 100 μm wide PDMS microchannels, each separated by 100 μm, permit the delivery of various solutions to the nanohole array sensors. The PDMS microchannels each include several arrays with periodicities ranging from 380 nm to 420 nm. Figure 7b shows a transmission mode image, where each spot's intensity can be monitored in real time. Figure 7c shows an SEM image of a single nanohole array sensing element, the same as in figure 1a.

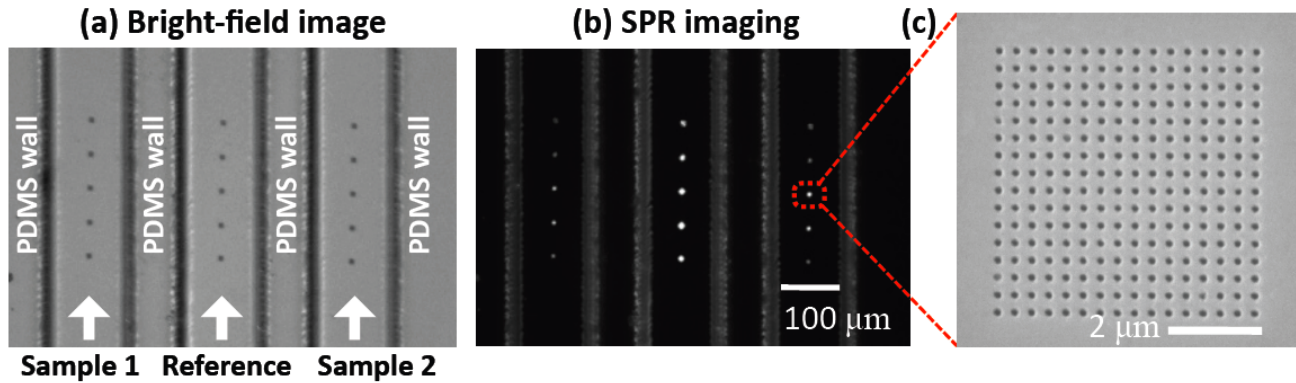


Fig. 7. CCD images of 3 parallel microfluidic channels permitting the delivery of different solutions to different nanohole array sensors. a) Bright-field image in reflection mode. b) Transmission mode image using a 10× microscope objective. The arrays are illuminated by a 633 nm HeNe laser beam. c) SEM image of one arrays of nanoholes.

Figure 8a shows measurements obtained by sequentially filling a PDMS microchannel with different mixtures of ethanol in water, thereby changing the bulk refractive index. The highest measured variation was obtained for the nanohole array with a 400 nm periodicity: as the refractive index changed from 1.333 to 1.353, the transmitted intensity dropped by 32%. Transmission through a nanohole array with a 420 nm periodicity is nearly flat, since the transmission spectrum is being sampled around a local minimum, i.e. the slope ($dI_T/d\lambda$) is close to zero.

Figure 8b presents real-time streptavidin-biotin specific binding measurements. On the gold surface, 4 mM of 11-amino-1-undecanethiol hydrochloride was first immobilized to form a self-assembled monolayer (SAM) over a 24 hour period, followed by the immobilization of 3 mM sulfo-NHS-LC biotin over a 12 hour period. The gold surface was then treated with bovine serum albumin (BSA) to reduce non-specific binding of proteins on the surface. Since no specific binding can occur between the streptavidin and the SAM, a single PDMS microchannel without the immobilized biotin served as a negative control. During the first 40 minutes of the real-time measurements, the channels were filled with a phosphate buffered saline (PBS) solution to get a stable baseline. Then the 3-channel PDMS chip was used to deliver 3 μM streptavidin in PBS solution at a 2 μL/hr flow rate. This resulted in a quick drop of the transmitted intensity at minute 40, due to the refractive index change of the streptavidin solution versus the PBS buffer. From minute 42, the intensity variation is due to the specific binding of the streptavidin to the biotin. The trend is exponential, which is characteristic of such first-order molecular interaction kinetics [35]. As the streptavidin-biotin reaction saturates, the transmitted intensity stabilizes.

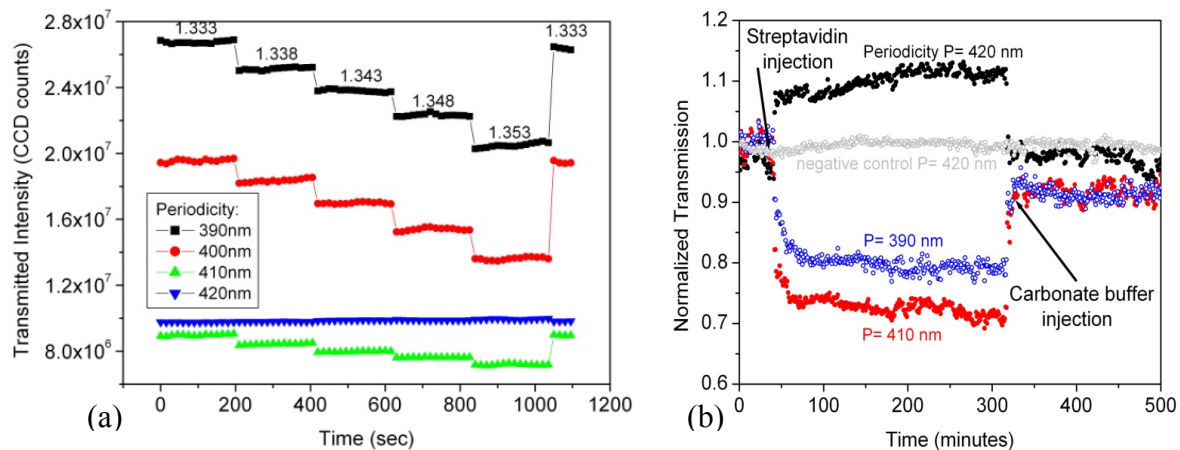


Fig. 8. a) Continuously measured transmission intensity, which depends on the bulk refractive index change due to various ethanol in water solutions and on the periodicity of the nanohole arrays. b) Real-time streptavidin-biotin binding kinetics measurement. For $(dI_T/d\lambda) < 0$, the intensity increases, as with the 420 nm periodicity nanohole array. For the others, $(dI_T/d\lambda) > 0$, and the intensity decreases.

4.5 Scaling issues for nanohole array SPR sensors

A nanohole-based microarray sensor system can be made highly parallel by tightly packing the nanohole array sensors and imaging the entire chip in a real-time high-throughput manner. Given the small size of $\sim 25 \mu\text{m}^2$, a 1 cm^2 microarray chip could theoretically contain more than 1,000,000 nanohole array sensors, giving the kind of high-throughput measurements needed for proteome-level investigations. Figures 9a and 9b show an implementation of a larger-scale microarray of periodic nanoholes. The 3-by-3 clusters of nanohole arrays are tightly packed and binding kinetics from each bright nanohole array sensor spot can be measured. However, high-density scaling presents several challenges. The current FIB fabrication method doesn't lend itself to large-area printing, but emerging technologies, such as nanoimprint lithography [36], or colloidal templating techniques [37], are able to print nanometer-sized patterns over centimeter-sized areas. Other challenges for scaling down the periodic nanohole microarray sensor include cross-talk and potential SP interference between neighboring nanohole array sensor elements, and poorer transmission resonances as the number of nanoholes within an array is reduced [38]. Recent work has shown the transfer of energy via SPs over several tens of microns between two separate nanohole arrays [39]. However, SP optical nanostructures provide many design freedoms, and with the addition of various SP optical elements [40], neighbor to neighbor cross-talk and interference can potentially be minimized [41]. Such work is currently under investigation.

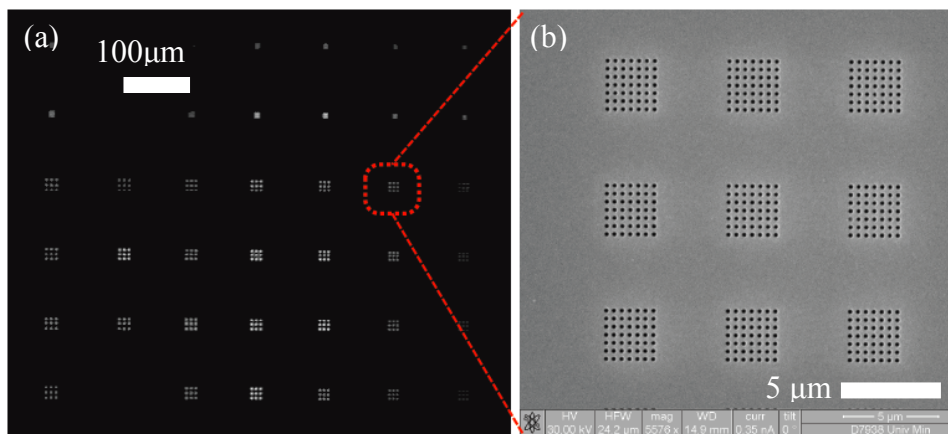


Fig. 9. (a) Laser transmission through a microarray of nanohole arrays. (b) In microarray spot, several nanohole arrays are tightly packed, spaced by $6 \mu\text{m}$.

5. CONCLUSIONS

In this work, we demonstrated a nanohole array based microarray system for real-time, high-throughput, label-free measurements of molecule-molecule surface binding events that offers several clear advantages over traditional SPR imaging techniques. The nanohole sensors in a microarray format provide the stability of a laser source, the sensitivity of SPR sensing, the scalability of traditional microarrays, and the simplicity of co-linear optics. Furthermore, the nanohole array design, the nanohole shape, and other novel SP optical elements offer many avenues for improving the sensitivity.

ACKNOWLEDGEMENTS

The authors gratefully acknowledge support from 3M Non-Tenured Faculty Award (S.-H. Oh), Minnesota Supercomputing Institute seed grant (A. Lesuffleur), 3M Science and Technology Fellowship (H. Im) and NIH Biotechnology Training Grant #T32-GM008347 (N.C. Lindquist). The authors also acknowledge Jennifer Maynard, Christy Haynes, and James Leger for helpful discussions. Device fabrication was performed at the University of Minnesota NanoFabrication Center, which receives support from the NSF National Nanotechnology Infrastructure Network (NNIN).

REFERENCES

- [1] B. Liedberg, C. Nylander and I. Lunström, "Surface plasmon resonance for gas detection and biosensing," *Sens. Actuators* **4**, 299 (1983).
- [2] M.A. Cooper, "Optical Biosensor in Drug Discovery," *Nat. Rev. Drug Discovery* **1**, 515 (2002).
- [3] R.H. Ritchie, "Plasma Losses by Fast Electrons in Thin Films," *Phys. Rev.* **106**, 874 (1957).
- [4] J. Homola, S.S. Yee and G. Gauglitz, "Surface plasmon resonance sensors: review," *Sens. Actuators B* **54**, 3 (1999).
- [5] N. Ramachandran, E. Hainsworth, B. Bhullar, S. Eisenstein, B. Rosen, A. Lau, J.C. Walter and J. LaBaer, "Self-assembling protein microarrays" *Science* **305**, 86 (2004).
- [6] E. Yeatman and E.A. Ash, "Surface-plasmon microscopy," *Electron Lett.* **23**, 1091 (1987).
- [7] B. Rothenhäusler and W. Knoll, "Surface-plasmon microscopy," *Nature* **332**, 615 (1988).
- [8] B.P. Nelson, A.G. Frutos, J.M. Brockman and R.M. Corn, "Near-infrared surface plasmon resonance measurements of ultrathin films. 1. Angle shift and SPR imaging experiments," *Anal. Chem.* **71**, 3928 (1999).
- [9] E.A. Smith and R.M. Corn, "Surface plasmon resonance imaging as a tool to monitor biomolecular interactions in an array based format," *Appl. Spectrosc.* **57** (11), 320A (2003).
- [10] E. Fu, J. Foley and P. Yager, "Wavelength-tunable surface plasmon resonance microscope," *Rev. Sci. Instrum.* **74** (6), 3182 (2003).
- [11] J.S. Shumaker-Parry, R. Aebersold and C.T. Campbell "Parallel, quantitative measurement of protein binding to a 120-element double-stranded DNA array in real time using surface plasmon resonance microscopy," *Anal. Chem.* **76**, 2071 (2004).
- [12] J.M. Brockman and S.M. Fernandez, "Grating-coupled surface plasmon resonance for rapid, label-free, array-based sensing," *American Laboratory* **33** (12) 37 (2001).
- [13] A.G. Brolo, R. Gordon, B. Leathem and K.L. Kavanagh, "Surface plasmon sensor based on the enhanced light transmission through arrays of nanoholes in gold films," *Langmuir* **20**, 4813 (2004).
- [14] S.M. Williams, K.R. Rodriguez, S. Teeters-Kennedy, A.D. Stafford, S.R. Bishop, U.K. Lincoln and J.V. Coe, "Use of the extraordinary infrared transmission of metallic subwavelength arrays to study the catalyzed reaction of methanol to formaldehyde on copper oxide," *J. Phys. Chem. B* **108**, 11833 (2004).
- [15] P.R.H. Stark, A.E. Halleck, D.N. Larson, "Short order nanohole arrays in metals for highly sensitive probing of local indices of refraction as the basis for a highly multiplexed biosensor technology," *Methods* (2005) 37.
- [16] K. Tetz, L. Pang and Y. Fainman, "High-resolution surface plasmon resonance sensor based on linewidth-optimized nanohole array transmittance," *Optics Letters* **31** (10), 1528 (2006)
- [17] A. De Leebeek, L.K.S. Kumar, V. de Lange, D. Sinton, R. Gordon and A.G. Brolo, "On-chip surface based detection with nanohole arrays," *Anal. Chem.* **79**, 4094 (2007).
- [18] A. Lesuffleur, H. Im, N.C. Lindquist and S.-H. Oh, "Periodic nanohole arrays with shape-enhanced plasmon resonance as real-time biosensors," *Appl. Phys. Lett.* **90**, 243110 (2007).
- [19] L. Pang, G.M. Hwang, B. Slutsky and Y. Fainman "Spectral sensitivity of two-dimensional nanohole array surface plasmon polariton resonance sensor," *Appl. Phys. Lett.* **91**, 123115 (2007).
- [20] A. Lesuffleur, H. Im, N.C. Lindquist, K. Lim and S.-H. Oh, "Laser-illuminated nanohole arrays for multiplex plasmonic microarray sensing," *Optics Express*, **16**, (1) 219 (2008).
- [21] J.V. Coe, J.M. Heer, S. Teeters-Kennedy, H. Tian and K.R. Rodriguez, "Extraordinary transmission of metal films with arrays of subwavelength holes," *Annu. Rev. Phys. Chem.* **59**, 179 (2008).
- [22] R. Gordon, D. Sinton, K.L. Kavanagh and A.G. Brolo, "A new generation of sensors based on extraordinary optical transmission," *Acc. Chem. Res.*, ASAP (2008).
- [23] T.W. Ebbesen, H.J. Lezec, H.F. Ghaemi, T. Thio and P.A. Wolff, "Extraordinary optical transmission through subwavelength hole arrays," *Nature* **391**, 667 (1998).
- [24] L. Martin-Moreno, F.J. Garcia-Vidal, H.J. Lezec, K.M. Pellerin, T. Thio, J.B. Pendry and T.W. Ebbesen, "Theory of extraordinary optical transmission through subwavelength hole arrays," *Phys. Rev. Lett.* **86**, 1114 (2001).
- [25] C. Genet, M. P. van Exter, and J. P. Woerdman, "Fano-type interpretation of red shifts and red tails in hole array transmission spectra," *Opt. Commun.* **225**, 331 (2003).
- [26] M. Sarrazin, J. P. Vigneron, and J. M. Vigoureux, "Role of Wood anomalies in optical properties of thin metallic films with a bidimensional array of subwavelength holes," *Phys. Rev. B* **67**, 085415 (2003).
- [27] H.J. Lezec, T. Thio, "Diffracted evanescent wave model for enhanced and suppressed optical transmission through subwavelength hole arrays," *Opt. Express* **12**, 3629 (2004).

- [28] W. L. Barnes, W. A. Murray, J. Dintinger, E. Devaux and T. W. Ebbesen, "Surface plasmon polaritons and their role in the enhanced transmission of light through periodic arrays of subwavelength holes in a metal film," *Phys. Rev. Lett.* **92**, 107401 (2004).
- [29] H.W. Gao, J. Henzie, T.W. Odom, "Direct evidence for surface plasmon-mediated enhanced light transmission through metallic nanohole arrays," *Nano Lett.* **6**, 2104 (2006).
- [30] H. Liu and P. Lalanne, "Microscopic theory of the extraordinary optical transmission," *Nature* **452**, 728 (2008).
- [31] Y. Xie, A.R. Zakharian, J.V. Moloney and M. Mansuripur, "Transmission of light through slit apertures in metallic films," *Opt. Express* **12**, 6106 (2004).
- [32] T.M. Chinowsky, T. Mactutis, E. Fu and P. Yager, "Optical and electronic design for a high performance surface plasmon resonance imager," *Smart Medical and Biomedical Sensor Technology, Proceeding of SPIE 5261 173* (2004) doi: 10.1117/12.538536
- [33] L.S. Jung, C.T. Campbell, T.M. Chinowsky, M.N. Mar and S.S. Yee, "Quantitative interpretation of the response of surface plasmon resonance sensors to adsorbed films," *Langmuir* **14**, 5636 (1998).
- [34] Y.N. Xia and G.M. Whitesides, "Soft lithography," *Angew. Chem. Int. Ed.* **37**, 550 (1998).
- [35] N. M. Green, "Avidin and Streptavidin," *Methods Enzymol.*, **184**, 51-67 (1990).
- [36] S. Y. Chou, P R. Krauss, and P. J. Renstrom, "Imprint of sub-25 nm vias and trenches in polymers," *Appl. Phys. Lett.* **67** (21), 3114 (1995)
- [37] C.-H. Sun, W.-L. Min and P. Jiang, "Templated fabrication of sub-100 nm periodic nanostructures," *Chem. Commun.*, 3163 (2008).
- [38] F. Przybilla, A. Degiron, C. Genet, T. W. Ebbesen, F. de Léon-Pérez, J. Bravo-Abad, F. J. García-Vidal, L. Martín-Moreno, "Efficiency and finite size effects in enhanced transmission through subwavelength apertures," *Optics Express* **16** (13), 9571 (2008)
- [39] E. Devaux, T. W. Ebbesen, J.-C. Weeber, and A. Dereux, "Launching and decoupling surface plasmons via microgratings," *Appl. Phys. Lett.* **83**, 4936 (2003).
- [40] N. C. Lindquist, A. Lesuffleur, and S.-H. Oh, "Periodic modulation of extraordinary optical transmission through subwavelength hole arrays using surrounding Bragg mirrors," *Phys. Rev. B* **76**, 155109 (2007).
- [41] N. C. Lindquist, A. Lesuffleur, and S.-H. Oh, "Lateral confinement of surface plasmons and polarization-dependent optical transmission using nanohole arrays with a surrounding rectangular Bragg resonator," *Appl. Phys. Lett.* **91**, 253105 (2007).